



Radiocarbon analysis confirms annual periodicity in *Cedrela odorata* tree rings from the equatorial Amazon

Guaciara M. Santos ^{a,*}, Daniela Granato-Souza ^{b,c}, Ana Carolina Barbosa ^b, Rose Oelkers ^d, Laia Andreu-Hayles ^d

^a Earth System Science, University of California, Irvine, B321 Croul Hall, Irvine, CA, 92697-3100, USA

^b Department of Forest Sciences, Federal University of Lavras, Lavras, MG, 37200-000, Brazil

^c Department of Geosciences, University of Arkansas, Fayetteville, AR, 72701, USA

^d Lamont-Doherty Earth Observatory of Columbia University, Palisades, NY, 10964, USA



ARTICLE INFO

Keywords:

Cedrela odorata
Tropical dendrochronology
Radiocarbon (^{14}C)
Bomb pulse dating (BPD)
Amazon basin
Inter tropical convergence zone
Equatorial line

ABSTRACT

A *Cedrela odorata* tree ring width chronology spanning from 1786 to 2016 was developed in the quasi-equatorial eastern Amazon Basin. Annual calendar dates were assigned using dendrochronological techniques at the Federal University of Lavras, Brazil. Due to its strategic location at the edge of the Equator (approximately $0^{\circ}57'\text{S}$), an independent confirmation of the annual periodicity of this century-long chronology would be of great value, allowing its future use for climate reconstruction and for filling gaps in upcoming atmospheric radiocarbon (^{14}C) compilations. For reconstruction of atmospheric ^{14}C , high reliability of the dendrochronological calendar dates is a requirement. Here, we used high-precision ^{14}C bomb pulse dating (BPD) of selected *C. odorata* tree rings as a robust independent method to validate the dendrochronological dates. Eight calendar years from across the pre-to post-bomb period were tested through ^{14}C analysis of α -cellulose extracts (19 targets in total were produced from those 8 calendar years). All dendrochronologically dated tree rings measured produced ^{14}C values in perfect alignment with the Southern Hemisphere ^{14}C bomb curve, further confirming the annual growth of this important record. Extraction of α -cellulose was attained by a recently implemented procedure at the Lamont-Doherty Earth Observatory (LDEO). The method was ^{14}C assessed by high-precision measurements at the Keck Carbon Cycle Accelerator Mass Spectrometer (KCCAMS) at the University of California, Irvine (UCI) by measuring reference materials and unknown samples. High reproducibility of reference materials (within uncertainties) showed that the novel 150-funnel system and protocol developed at LDEO is reliable and can potentially expedite cellulose extractions for ^{14}C analysis.

1. Introduction

The Amazon Basin is one of the world's largest convective centers and plays an important role in the hydrological dynamics of tropical South America (Vera et al., 2006; Nobre, 2014). This humid forest not only maintains megadiverse flora and fauna but also brings massive amounts of moisture to continental parts of South America; in south-central Brazil, for instance, this moisture sustains one of the most productive areas of the country (Marengo and Soares, 2004; Nobre, 2014). The tropical Pacific and Atlantic oceans are the main climate drivers that modulate the interannual variability of the Amazonian hydrological cycle (Vera et al., 2006; Yoon and Zeng, 2010). Recent studies have reported and forecasted significant hydroclimate shifts all over the

Amazon Basin (Marengo and Espinoza, 2016). Thus, there is an urgent need for reliable paleoclimate data from the recent past to validate how unprecedented these anticipated changes are in the context of climate change.

Moisture-sensitive tree-ring chronologies can provide reliable climatic reconstructions and have been widely and successfully used in the middle latitudes (Villalba et al., 1998; Fritts, 2001; Villanueva-Diaz et al., 2007; Griffin et al., 2013; Stahle et al., 2011, 2016). In the moist tropics it has been a challenge to find native tree species that can be dated to their calendar year of formation; however, dendrochronological studies have shown promising results in the middle to lower latitudes (Worbes, 1984, 1985; Villalba et al., 1985; Schöngart, 2008; Rozendaal and Zuidema, 2011; Brienen et al., 2016), and efforts are now

* Corresponding author. Department of Earth System Science, University of California, Irvine, Irvine, CA, USA.
E-mail address: gossant@uci.edu (G.M. Santos).

under way to describe hydroclimatic variability over the Amazon Basin through the study of annual growth rings (Schöngart et al., 2004; Bräuning et al., 2009; Lopez and Villalba, 2011; López et al., 2017; Granato-Souza et al., 2018a). A recent rainfall reconstruction using tree-ring data from *Cedrela odorata* was developed at the Rio Paru State Forest in the quasi-equatorial Amazon Basin (Fig. 1) through a collaboration between the Federal University of Lavras (Brazil) and the University of Arkansas (USA). This *C. odorata* tree-ring chronology represents one of the most relevant paleoclimate proxies in the Equator since it exhibits annual resolution, overlaps with meteorological data during the calibration period, and covers back to the end of the 18th century in a region where instrumental data is scarce, short, and discontinuous (Granato-Souza et al., 2018a). This century-long *C. odorata* chronology is already contributing to the International Tree Ring Data Bank (ITRDB) at NOAA's Paleoclimatology Program (Granato-Souza et al., 2018b; BRA001). This record is moisture-sensitive and exhibits a significant relationship with Sea Surface Temperatures (SST) from both the tropical Atlantic and Equatorial Pacific. The regional climatic signal and large-scale connections recorded by the Rio Paru *Cedrela* chronology represent a climatological breakthrough in one of the most remote and unknown parts of the eastern Amazon Basin (Granato-Souza et al., 2018a).

The presence of annual growth rings in trees from subtropical and tropical humid forests has been discredited for a long time (Worbes, 2002; Dünisch et al., 2003) and remains a cause of debate. Poorly-defined anatomical features (such as vague, discontinuous, false, and absent tree rings) have been detected in *Juniperus procera* from Ethiopia (Wils et al., 2009), *Pseudolmedia rigida* from Bolivia (Andrew-Hayles et al., 2015), *Priaria copaifera* from Colombia (Herrera-Ramirez et al., 2017), and two Australian subtropical *Araucariaceae* species

(Haines et al., 2018). The lack of seasonality has been pointed out as the main cause, of the nonexistence and/or irregularity of annual tree-ring formation in the tropics (Baker et al., 2017). However, many studies have proposed different mechanisms by which annual tree rings in ~200 tropical species can be triggered. They are rainfall seasonality, annual flooding, soil water salinity (mangroves), and/or changes in the photoperiod and temperature in higher latitudes and altitudes (Schöngart et al., 2017). Overall, it seems that a wide variety of responses have been observed for tropical trees, and that the presence of annual periodicity in tree growth is very much dependent on site environmental variability and particular tree species features.

The well-formed and concentric growth rings found in the *C. odorata* samples from the Rio Paru site (Fig. 1) were crossdated using skeleton plots and visually dated under a microscope (Douglass, 1941; Stokes and Smiley, 1996). The dated ring widths were precisely measured (0.001 mm), and the dating accuracy was checked with the computer program COFECHA (Holmes, 1983). Standard dendrochronological techniques primarily indicated the annual formation of the sample's growth rings. Annual resolution was further confirmed with climate analysis, where synchronous behavior was found between the Rio Paru chronology and instrumental climate data (Granato-Souza et al., 2018a). Still, annual ring formation in wet tropical forests has been shown to be challenging, even when the ring width variations appear to be related to climate variability (e.g., Herrera-Ramirez et al., 2017). Moreover, a recent report has shown that *C. odorata* trees growing near Matapi, Surinami (approximately 4° N of the Rio Paru State Forest; Fig. 1), formed two rings per year, suggesting that annual growth ring formation is related to site seasonality and not dependent only on tree species biology (Baker et al., 2017). For the reasons described above, an assessment of the periodicity of wood formation by an independent dating method such as

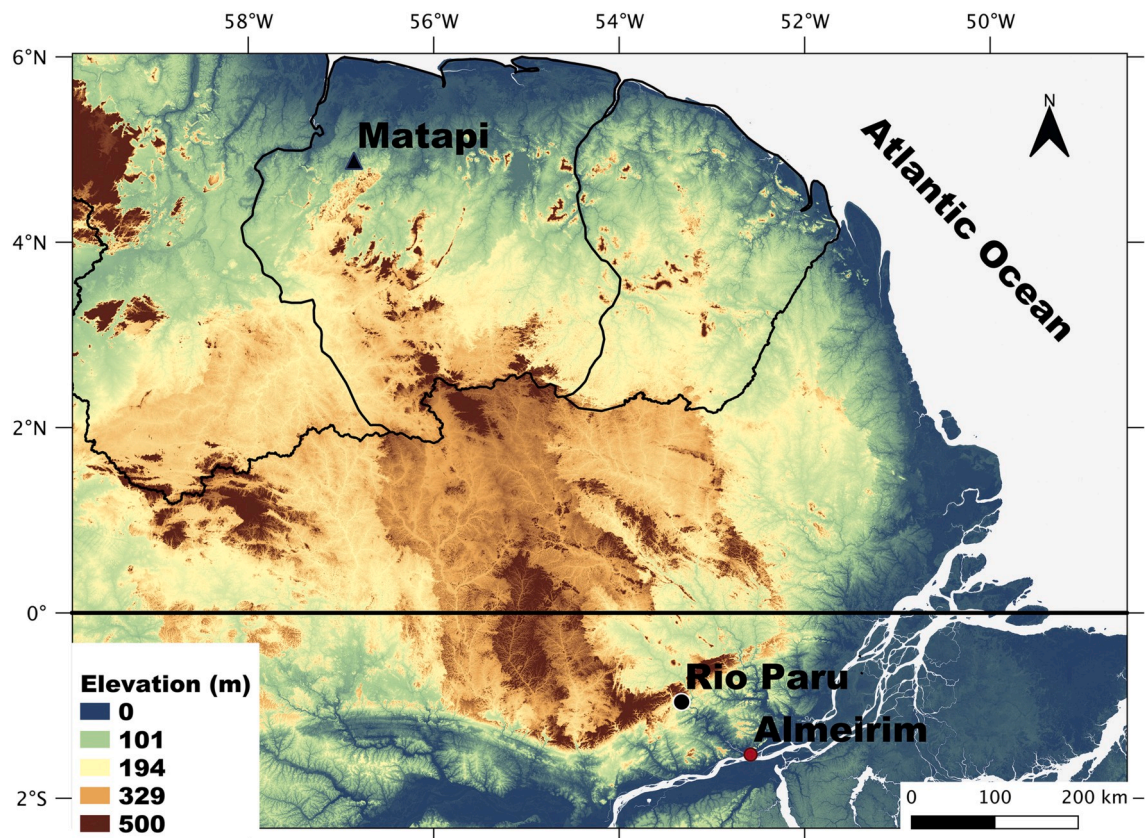


Fig. 1. Map of the study area that shows Rio Paru site (black circle) in the Eastern Equatorial Amazon, Brazil, where cross-sections from *Cedrela odorata* have been taken; the Matapi site (black triangle) shown in Baker et al. (2017) and Almeirim (red circle), the closest municipality to the Rio Paru site. The range of colors from blue to red represents altitude changes from sea level to the highest elevation level in meters. (For interpretation of the references to color in this figure legend, the reader is referred to the Web version of this article.)

radiocarbon (^{14}C) bomb pulse dating (BPD) would assert the value of this annually resolved chronology and allow further applications of this climate proxy.

The ^{14}C BPD method takes advantage of the ^{14}C bomb-peak and provides an unambiguous approach to directly verify the calendar years determined by dendrochronological techniques using the ^{14}C signatures fixed in organic tissues after 1950 (as fraction modern carbon – F ^{14}C ; Reimer et al., 2004). During photosynthesis, trees fix atmospheric $^{14}\text{CO}_2$ in their cellulose fibers, an important structural component of wood. The ^{14}C signature measured in tree-ring cellulose can be a reliable proxy of atmospheric $^{14}\text{CO}_2$. The excess of atmospheric $^{14}\text{CO}_2$ from the advent of nuclear weapons testing in the early 20th century — i.e., starting in 1952 with the Eniwetok Atoll test “Mike,” Marshall Islands, Pacific Ocean (Kutschera 2018)—almost doubled the ^{14}C concentration in Earth’s atmosphere. Soon after the test ban treaty in 1963, the redistribution of the extra atmospheric ^{14}C among the major carbon reservoirs, coupled with CO_2 emissions from fossil fuel combustion (F ^{14}C = 0), shaped the ^{14}C bomb pulse. While nowadays the bomb pulse has mostly faded away, this anthropogenic marker can still be found in all long-living organisms that overlap in the timelines of the early bomb nuclear tests (i.e., last 70 years).

The isolation of post-AD 1950 ^{14}C signatures in organic tissues, once matched with the ^{14}C signal from early pre-established atmospheric $^{14}\text{CO}_2$ curves (e.g., Levin and Hesshaimer, 2000; Levin et al., 2008, 2013), can help to determine the calendar years of tissue formation (Santos, 2012; Kutschera, 2018, and references therein). When the calendar year of the material tested has been inferred by other means (such as historical records or dendrochronological dating, for example), the ^{14}C BPD method can be an independent validation of the records’ dates with a precision of approximately 1 year or less (depending on the time of formation of the material tested and its specific timeframe). The BPD method has been used successfully for testing tree-ring periodicity of tree species under distinctive environments, such as subtropical and tropical areas in Mexico (Biondi and Fessenden, 1999; Beramendi-Orsco et al., 2018), Costa Rica (Fichtler et al., 2003), Panama (Westbrook et al., 2006), Australia (Pearson et al., 2011; and Haines et al., 2018), Africa (Worbes et al., 2003; Wils et al., 2009; Groenendijk et al., 2014), Argentina (Hadad et al., 2015), southeastern Brazil (Santos et al., 2015), and several areas along the Amazon Basin and Andean forest (Andreu-Hayles et al., 2015; Ohashi et al., 2016; Herrera-Ramirez et al., 2017; Baker et al., 2017; de Miranda et al., 2018). Inconsistent dendrochronology dates from tree species previously disclosed as annual have also been effectively determined by the BPD method (e.g., Soliz-Gamboa et al., 2011; Groenendijk et al., 2014; Herrera-Ramirez et al., 2017; Baker et al., 2017). Ideally, more than just one calendar year (Geraldo Jimenez and del Valle, 2011) should be tested to avoid an incorrect initial conclusion about the dendrochronology dating (see details in Herrera-Ramirez et al., 2017). Coupling ^{14}C measurements with dendrochronological techniques has also allowed underestimation and/or systematic overestimation of calendar ages by cross-dating to be properly corrected. For instance, Fichtler et al. (2003) detected missing tree rings on tree species of Costa Rica, while Baker et al. (2017) detected biannual ring formation in Suriname. Nonetheless, it is imperative that the correct structural wood extract (holocellulose or α -cellulose) be analyzed by ^{14}C (Cain and Suess, 1976; Leavitt and Bannister, 2009). Otherwise results can be biased by mobile carbon from previous years (Worbes and Junk, 1989; Westbrook et al., 2006).

To capture high excursions of $^{14}\text{CO}_2$ in the Earth’s atmosphere, researchers require high-resolution existing monthly or annual ^{14}C records measured in air samples. However, these records are temporally short and geographically scarce (Hua et al., 2013). The oldest and more consistent in situ CO_2 measurements belong to the Wellington site in New Zealand at 41°S (Turnbull et al., 2017). Furthermore, this is the only Southern Hemisphere (SH) record that shows direct monthly ^{14}C data during the entire bomb spike.

Currently, post-AD 1950 atmospheric ^{14}C is divided into inter-

hemispheric zones defined in Hua et al. (2012, 2013): NH1, NH2, and NH3 curves for the Northern Hemisphere, and the SH1-2 and SH3 curves for the Southern Hemisphere. These observational post-AD 1950 ^{14}C datasets are of critical importance for synchronizing multiple lines of proxy evidence, including contributions to global carbon budget assessment (i.e., carbon’s distribution among reservoirs), determination of a regional present-day baseline to access ground-based fossil fuel CO_2 emissions, as well as helping with applications to forensic sciences (Kutschera, 2018, and references therein). Moreover, post-AD 1950 ^{14}C datasets may potentially be useful for investigating long-term responses of cumulative drought effects in trees. Induced absence of wood production in trees associated with extreme climate events has already been reported (Novak et al., 2016).

As of today, ^{14}C records are missing at sites across the Intertropical Convergence Zone (ITCZ) and especially from the western portion of the SH (Santos et al., 2015). To complete an atmospheric ^{14}C global dataset that better illustrates the geographical particularities and atmospheric circulation affecting ^{14}C distribution, further records based on precise dendrochronological data are needed.

This work’s primary goal is to independently validate the annual resolution of the Rio Paru *cedrela* chronology (Granato-Souza et al., 2018a). If the annual growth-signal of tree rings in *C. odorata* from equatorial Amazon can be demonstrated by high-precision ^{14}C BPD, this important dendrochronological record also can potentially be selected to participate in the novel atmospheric ^{14}C compilation proposed by Santos et al. (2015, 2019). A secondary goal is to extend the application of a newly developed α -cellulose extraction method (Andreu-Hayles et al., 2019). Until now this method has been used exclusively for measurements of $\delta^{18}\text{O}$ and $\delta^{13}\text{C}$ signatures in tree rings. This new extraction protocol has the benefit of being relatively efficient while dealing with a large number of samples. Therefore, introducing this methodology into the ^{14}C dating of tree-ring samples is expected to expedite ^{14}C analysis while producing sufficient amounts of material for stable isotope measurements.

2. Materials and methods

2.1. Site, sample selection, and strategies

Cross-sections of *C. odorata* were obtained from legal logging operations at the Paru State Forest (53.326°W; 0.979°S), which comprises an area of 3.6 mi ha, located north of the Amazon River and near the southern escarpment of the Guiana Highlands (Fig. 1). This humid and undisturbed dense forest is close to the municipality of Almeirim, located at the northernmost part of the Brazilian state of Pará. Almeirim has a very low population density (0.5 inhabitants/km 2), and therefore local anthropogenic fossil CO_2 contributions to our site are negligible. Our study site, located at the tropical rainbelt across the Equator (Fig. 1), is most likely influenced by the north-south movements of the ITCZ and by the El Niño Southern Oscillation (ENSO) (Garreaud et al., 2009). Based on observational data obtained from the CRU TS4.00 0.5° gridded dataset from 1939 to 2016 (see details in Granato-Souza et al., 2018a), the climate in this location (5°N–5°S, 60°–53°W) is characterized by high annual temperatures averaging about 27.2 °C and relatively high precipitation throughout the year, with about 1970 mm annually. Two well-defined seasons (Fig. 2) are present, with the wettest period usually starting in December and extending to the end of July (average of ~286 mm), and a short dry season spanning from August to November (average of ~67 mm). Recent climate-growth relationship analysis (Granato-Souza et al., 2020) indicates that the growing season in the Paru site (Fig. 1) spans from February to July (green bar in Fig. 2).

The fully replicated *C. odorata* chronology from 1786 to 2016 was constructed based on 56 radii from 27 trees (Granato-Souza et al., 2018a). The wood sections presented exceptionally clear tree rings with very well-defined boundaries, and the individual ring-width series patterns were easily matched among trees. At this location *C. odorata*’s

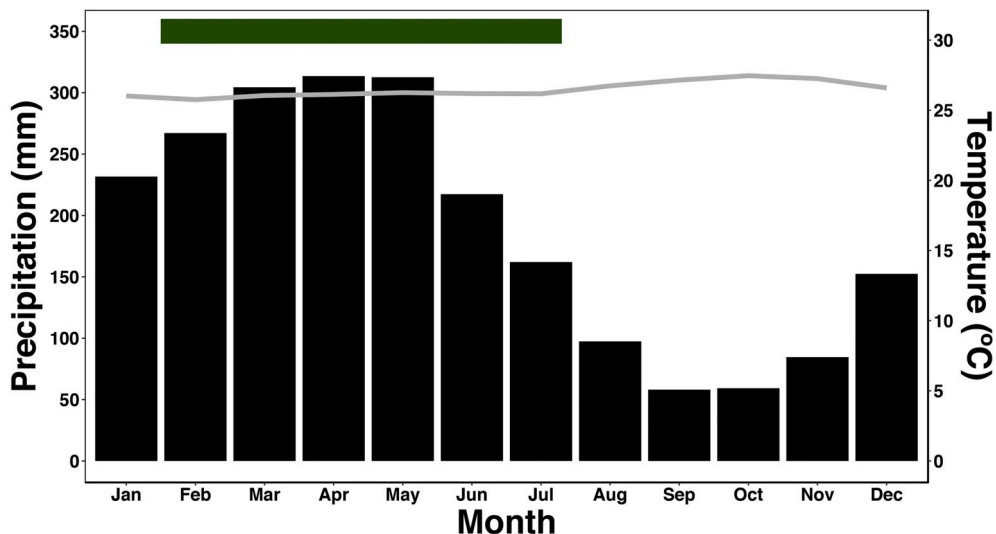


Fig. 2. Climate diagram showing monthly average temperature (gray line) and monthly precipitation (black bars) from monthly climate gridded data extracted from CRU TS4.00, (5°N–5°S, 60°–53°W). Green bar represents the estimated growth period based on climate-growth relationship analysis (Granato-Souza et al., 2020). (For interpretation of the references to color in this figure legend, the reader is referred to the Web version of this article.)

wood anatomy has thin marginal parenchyma bands and semi-porous vessels, as shown in the high-resolution wood image from the scan of the sample that was used in this study (Fig. 3). From this tree cross-section, eight rings were selected from 1940 to 2016 for ^{14}C BPD growth periodicity validation. The dendrochronological calendar years of the eight *C. odorata* rings selected for ^{14}C sample processing and measurements were 1940, 1946, 1956, 1960, 1964, 1969, 1979, and 1999. While the calendar years of 1940 and 1946 are not from the ascending or descending slopes of the ^{14}C BPD, their respective wood material was selected to ensure that the chemical extraction procedure adopted isolated the proper carbon fraction to be ^{14}C measured (i.e., structural carbon, as recommended by Cain and Suess [1976] and Leavitt and Bannister [2009]).

Non-structural carbon compounds (NSC), primary sugars and starches, are vital to plants (Adams et al., 2017). They can accumulate within plant tissues for future usage in tissue regrowth or post-stress recovery and repair (Furze et al., 2019, and references therein). The transport of NSC from previous years in wood tissue can bias ^{14}C determinations. Worbes and Junk (1989) reported skewed ^{14}C results when measuring minimally chemically treated wood (i.e., samples were pretreated with 2% HCl and 2% NaOH solutions before liquid scintillation beta spectrometry measurements took place). Thus, the standard pretreatment acid-base-acid (ABA; Santos and Ormsby, 2013) is not recommended for non-fossil wood samples, as previously determined by Cain and Suess (1976). Incomplete removal of resinous compounds has been detected in post-bomb *Hymenaea courbaril* from Panama when ABA-treated tree rings were measured by ^{14}C (Westbrook et al., 2006). Therefore, only holocellulose or α -cellulose chemical extraction

procedures are normally acceptable for isolating structural carbon for post-bomb tree-ring/ ^{14}C dating studies (Santos et al., 2015; Hadad et al., 2015; Andreu-Hayles et al., 2015; Baker et al., 2017, for example).

Another systematic type of potential ^{14}C bias refers to the mechanical separation of the annual growth rings. To ensure that the full growing season was sampled without losing material from the growing season of interest or including material from neighboring rings, the short subset of 8 tree rings from *C. odorata* was measured in replicates. Such precaution provides ^{14}C measurement accuracy and precision, but also allows us to evaluate the unbiased ^{14}C signal of tree rings in *C. odorata* from the equatorial Amazon. If this tree species at this location is truly annual, as expected, the trees from this dendrochronological record can be further used to fine-tune post-bomb atmospheric ^{14}C reconstructions, as suggested by Santos et al. (2015, 2019).

2.2. Laboratory procedures

2.2.1. Cellulose extraction method at LDEO

Recently researchers at the LDEO developed and implemented a new method for α -cellulose extraction from wood samples for stable isotope analyses of $\delta^{18}\text{O}$ and $\delta^{13}\text{C}$ signatures (Andreu-Hayles et al., 2019). This process included constructing polytetrafluoroethylene (PTFE-Teflon) devices to hold the samples in individual homemade funnels, allowing for the extraction of α -cellulose from 150 wood samples per batch with minimal manipulation. The use and disposal of chemicals were optimized using an Erlenmeyer flask connected to a vacuum pump, which increased the efficiency of the overall procedure while reducing the amount of chemicals needed. The procedure's timing efficiency, after

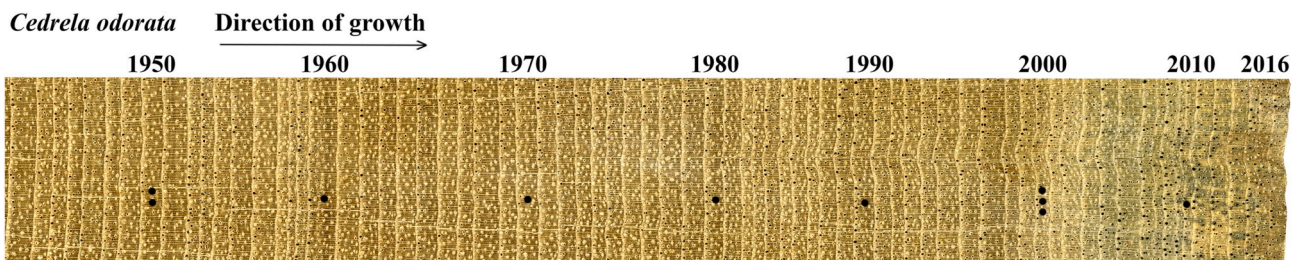


Fig. 3. Transverse section view of the *C. odorata* wood fragment selected for ^{14}C BPD. The wood anatomy of the tree rings is formed by semi-ring porosity and marginal parenchyma. Furthermore, significant differences in ring widths along the wood sample's radial direction can be observed. This ring-width variability was associated with variations in rainfall strength (Granato-Souza et al., 2018a).

loading wood samples in the apparatus, has exceeded previous protocols' (e.g., Leavitt and Danzer, 1993).

While the α -cellulose extraction method at LDEO has proven to be efficient in removing extractives, lignin, and hemicellulose for stable isotopic analysis (Andreu-Hayles et al., 2019), careful assessment of any chemical protocol must be made for ^{14}C applications (Santos et al., 2010). Furthermore, the use of acetic acid as buffer, coupled with a rapid α -cellulose chemical extraction, has been shown to introduce biases to ^{14}C data (Anchukaitis et al., 2008). To verify whether the new method could be used in high-precision ^{14}C analysis, we first tested randomized unanimous ^{14}C value agreements of known-aged materials. For that, KCCAMS/UCI shipped a suite of reference materials ranging from ^{14}C -free ($\text{F}^{14}\text{C} = 0$) to post-bomb values ($\text{F}^{14}\text{C} > 1$). Table 1 describes the reference materials exchanged. The eight dendrochronologically dated tree-ring samples of *C. odorata* selected for this study (i.e., years 1940, 1946, 1956, 1960, 1964, 1969, 1979, and 1999, as mentioned earlier) were also shipped from KCCAMS/UCI to LDEO with enough wood material to produce replicates.

Upon arrival at LDEO, all samples were stored in an electronic desiccator in the Terrestrial Ecology Laboratory for approximately 24 h. To have enough α -cellulose material for ^{14}C analyses, at least 20 mg of raw material per reference material and wood samples were weighed out. Although IAEA-C3 is already in cellulose form, it was also exposed to the same chemical treatments. Before chemical extractions started, wood samples were chopped into fine fibers using a #20 Feather disposable stainless-steel surgical blade, except barley mash FIRI-J, which is already flaked. The wood material was placed in individual funnels to undergo several chemical treatments. The LDEO custom-designed α -cellulose extraction system is composed of 150 funnels throughout 3 polytetrafluoroethylene (PTFE-Teflon) devices placed inside a controlled-heated water bath. Chemicals are poured manually inside the funnels and are drained through a tube connected to an

Erlenmeyer flask that connects to the vacuum pump for waste disposal, as mentioned earlier. Reference materials and wood samples withstand an intensive 2-day chemical extraction treatment, as follows: six 1-h baths of sodium chloride (NaClO_2) at 80 °C; two 45-min baths of sodium hydroxide (NaOH) in 10% and 17% concentrations at 70 °C and room temperature, respectively; and two 1-h baths of sodium chloride (NaClO_2) at 80 °C. Per the Andreu-Hayles et al. (2019) chemical protocol, the chlorination/bleaching steps also use acetic acid ($\text{CH}_3\text{CO}_2\text{H}$) as buffer. The second chlorination/bleaching step takes place between the NaOH treatments and the rinsing sessions with ultrapure water ($\sim 18 \text{ M}\Omega\text{cm}$). To adjust this chemical protocol for ^{14}C analyses and therefore remove any possibility of ^{14}C results being biased by $\text{CH}_3\text{CO}_2\text{H}$ residues (attached in the final product), an additional final treatment of 1N HCl 70 °C for 30 min was applied before ultra-pure water rinses took place. All samples, with the exception of IAEA-C3, were later homogenized using Fisher Scientific FS20 ultrasonic bath. Post-homogenization, cellulose samples were kept frozen for at least 24 h, and then freeze-dried for another 24 h. Dried samples were stored in an electronic desiccator prior to shipment to the KCCAMS/UCI facility. Replicates were produced from both "raw" wood fine fibers and α -cellulose extracts after finalizing the entire protocol.

2.2.2. Radiocarbon sample processing and analytical procedures at KCCAMS/UCI

Radiocarbon measurements were conducted on graphite targets. To produce filamentous graphite, α -cellulose extracts were first converted to carbon dioxide (CO_2) in evacuated sealed quartz tubes loaded with purified copper oxide (CuO) at 900 °C for 3 h. Individual CO_2 samples were then cryogenically purified and reduced to graphite over 5 mg of pre-reduced iron catalyst in graphitization vessels following established protocols (Santos and Xu, 2017). Filamentous graphite was loaded into aluminum (Al) target holders and measured at an in-house modified AMS compact instrument (Beverly et al., 2010).

High-precision ^{14}C measurements were attained by cycling injections of masses of carbon 12, 13, and 14 through the spectrometer, and by offline isotopic fractionation correction loop-by-loop using the measured $^{13}\text{C}/^{12}\text{C}$ data (i.e., the derived $\delta^{13}\text{C}$) of the corresponding $^{13}\text{C}/^{12}\text{C}$. The direct online- $\delta^{13}\text{C}$ isotopic fractionation correction enhances ^{14}C values, as machine fractionation effects affecting ratios can be amended (Santos et al., 2007). Multiple analyses of primary and secondary standards, as well as proper procedural background correction, allows for better measurement accuracy and precision (Santos et al., 2010). A suite of reference materials (described in Table 1) granted the evaluation of the novel α -cellulose extraction protocol recently implemented at LDEO. Note that most of the aforementioned reference materials were subject to the same chemical α -cellulose extraction steps of the LDEO protocol, so that proper procedural blank and accuracy assessment could be determined. Additional targets from the same set, undergoing conventional laboratory sample preparation procedures, enable quality control tests. Graphite targets produced from oxalic acids (OX-I and II), the sucrose (ANU), and the USGS POC coal (Santos et al., 2007, 2010) were ^{14}C measured alongside cellulose extracted samples for spectrometer tuning and data normalization.

The ^{14}C results reported here are in terms of "Fraction modern carbon" or just F^{14}C , following the recommendation of Reimer et al. (2004). Individual errors reported were determined by taking into account factors such as counting statistics, primary and secondary standard measurement accuracy/precision, isotopic fractionation, and background corrections, as described in Santos et al. (2007).

3. Results and discussion

3.1. Reliability of the LDEO α -cellulose protocol for ^{14}C analysis

The results from the ^{14}C analysis for the reference materials shown in Table 1, after the LDEO α -cellulose extraction, are summarized in

Table 1
List of reference materials tested in this study and their relevant isotopic information.

Reference materials tested	Description	Origin	Consensus value (F^{14}C)	Citation
Queets-A	Fossil wood	Queets River mouth, Olympic Peninsula, WA	0.0011	Santos & Ormsby (2013)
AVR-07-Pal37	Fossil wood	Yukon, Central Alaska	0.0011	Reyes et al. (2010)
FIRI-D	Subfossil wood	Belfast Scots Pine (dedro-dated wood)	0.5705	Board (2002)
FIRI-H	Subfossil wood	Hohenheim oak (dedro-dated wood)	0.7574	Board (2002)
FIRI-J	Barley mash	N/A	1.0690	Board (2002)
IAEA-C3	Extracted cellulose	1989 growth season sampled from 40 trees	1.2941	Rozanski et al. (1992)
PS-76-86	Tree ring cross-section wedge	Mt. Decoeli, Kluane National Park, Canada	1900–1975 (50–200 yrs BP + post-bomb)	in-house standard

Queets-A and AVR-07-Pal37 are non-finite wood samples used as in-house blanks. The F^{14}C reported here are best values measured at KCCAMS/UCI, uncorrected for any type of background and published elsewhere. The selected FIRI samples are from the Fourth International Radiocarbon Intercomparison program, managed by Department of Statistics, Glasgow University (Scott, 2003). The pre-extracted cellulose IAEA-C3 is from the International Atomic Energy Agency. Finally, the PS-76-86 tree-ring cross-section wedge from Mt. Decoeli has been previously reported to have annual periodicity (Thomas W. Stafford Jr., per communication). Its site collection and correct tree species identity are unknown. Five calendar years were selected from this wedge and sampled for this study.

Table 2. To rule out internal variability during the sample processing and measurements, additional in-house samples were measured for comparisons. They were from the same original materials exchanged (Table 1), extracted as holocellulose or ABA, plus the untreated pre-extracted cellulose (i.e., IAEA-C3). Radiocarbon results from these extra samples were in close proximity to the expected values reported in Table 1, and therefore they are not mentioned further here. Fig. 4 illustrates the difference between the ^{14}C values obtained from the individual targets produced from the reference materials tested (Table 2) and consensus ^{14}C values (Table 1).

Regarding the procedural ^{14}C blank levels of the LDEO α -cellulose extraction protocol, we analyzed the ^{14}C content of several targets produced from two ^{14}C -free woods, Queets-A and AVR-07-Pal37. Their ^{14}C values were significantly higher than previously expected (Table 2; Fig. 4). The best result from a single target yielded a $F^{14}\text{C}$ of 0.0059 ± 0.00010 (equivalent to $41,240 \pm 150$ yrs BP) for Queets-A. This ^{14}C result is younger than those obtained by other methods (Santos and Ormsby, 2013, Table 1), indicating the presence of a fraction of “modern” contamination (Santos et al., 2010). Considering that Queets-A is a fossil wood that tends to be digested quickly when subjected to cellulose extraction (Southon and Magana, 2010), our initial thought was that this blank material’s low ^{14}C performance was due to its wood preservation coupled with low cellulose yield recovery (Table 2) when just 20 mg of material was initially pretreated. The same LDEO α -cellulose extraction procedure was repeated to pretreat twofold more Queets-A and the second fossil wood listed in Table 1 (i.e., AVR-07-Pal37). Nonetheless, further ^{14}C results from larger wood extractions and/or from the well-preserved AVR-07-Pal37 fossil wood did not significantly improve cellulose yield recoveries or ^{14}C age results (Table 2). Therefore, the LDEO protocol is not suitable for unknown wood samples way beyond deglacial ages.

The subfossil woods FIRI-H and FIRI-D have consensus values of approximately 2232 yrs cal. BP (or 313–294 BC) and 4508 yrs cal. BP (or 3200–3239 BC), respectively. Therefore, they are ideal for evaluating accuracy and background correction in samples with less than 10 kyr BP (BP= Before Present or Before 1950). Furthermore, they can help to determine whether chemicals, tools, extraction apparatus, freeze-dryers, and desiccators are not introducing significant amounts of “younger exogenous carbon” to extracts, as these woods are notably old and highly sensitive to modern contamination as well (Santos et al., 2010). Good to excellent reproducibility was attained from the ^{14}C data produced for FIRI-H and FIRI-D, and although the measurement population here is relatively small (e.g., $n = 7$ and $n = 5$ for FIRI-H and FIRI-D, respectively), the data scatter was very low (Fig. 4 and Table 2).

To assess the reproducibility and accuracy of post-bomb materials, we tested the reference materials FIRI-J and IAEA-C3. Radiocarbon values’ deviations from their consensus value would indicate some type of fossil pollution contamination during sample processing (possibly from plastics in apparatus attachments, local atmospheric CO_2 , among others). While mean difference of our average FIRI-J ^{14}C value from its

consensus was less than 2.0% based on nine measurements, calibration with IAEA-C3 gave the highest deviation from the mean after 15 replications. The discrepancies observed from IAEA-C3 may be explained by features of the reference material itself. As the material is already distributed in its cellulosic form, we assumed that re-homogenization after chemical interaction (section 2.2.1) was unnecessary. According to the International Atomic Energy Agency (IAEA), this reference material was produced from one season’s harvest of ca. 40-year old trees from Sweden and bleached to cellulose at a paper factory. A recent work has reported a slightly higher mean value after multiple measurements of untreated IAEA-C3 cellulose (e.g., $F^{14}\text{C} = 1.298 \pm 0.001$; Wacker et al., 2010). If this certified reference material is not completely homogeneous, re-extracting larger amounts of it and running subsamples of it by high-precision ^{14}C will eventually lead to a larger scatter. Therefore, we believe that the ^{14}C results from FIRI-J barley better represent our procedure’s performance at the ^{14}C upper range (post-bomb period), as both precision and accuracy have been achieved upon full α -cellulose chemical extraction, and with a lesser number of measurements as well. Further tests using the IAEA-C3 reference material should be done to better clarify this issue.

To further assess the ability of the LDEO α -cellulose protocol when determining post-bomb calendar ages from tree rings, we also selected five calendar years from a wood wedge and measured them by high-precision ^{14}C in duplicates. The PS-76-86 wood cross-section came from a National Park located in the Yukon Territory at 60° N. Therefore, the PS-76-86 $F^{14}\text{C}$ values are plotted in Fig. 5 along with atmospheric CO_2 $F^{14}\text{C}$ values from the NH Zone 1 (Hua et al., 2013). The average and standard deviations of the ^{14}C dated five tree-ring pairs are shown in Table 3.

Overall, most of the ^{14}C values obtained for the selected tree rings of the Canadian PS-76-86 are similar to NH Zone 1 atmospheric values (Fig. 5). The pair of tree rings from the 1939 calendar year is also in agreement with expected pre-bomb $^{14}\text{CO}_2$ value (Fig. 5), ensuring that the novel α -cellulose extraction method (Andreu-Hayles et al., 2019) isolates mostly structural carbon and therefore is useful for ^{14}C analysis. If a small fraction of NSC from previous vegetation growth was still present in the α -cellulose extract, the $F^{14}\text{C}$ of 1939 would appear more enriched in ^{14}C than at expected atmospheric levels (Cain and Suess, 1976; Worbes and Junk, 1989).

While we cannot recommend the use of the LDEO α -cellulose method (Andreu-Hayles et al., 2019) for older ^{14}C age wood samples, this protocol seems suitable for samples within a large ^{14}C age spectrum (i.e., from Marine Isotope Stage 2 to present day). The ^{14}C results from all relevant reference materials (Table 2) are significantly indistinguishable from their expected values (Table 1), and have standard deviations of approximately 3% or less (Fig. 4). Note that they have been background-corrected by the average higher blank values (e.g., Queets-A and AVR-07-Pal37; Table 2; Fig. 4). A pooled standard deviation calculation (McNaught and Wilkinson, 1997) using the sets of replicated measurements (i.e., 6 reference materials and 5 cross-dated tree rings) suggests that the ^{14}C determination of uncertainty for this set of measurements is better than $\pm 2.2\%$.

3.2. Annual periodicity of the *C. odorata* growth at the Paru State Forest and its potential for future atmospheric ^{14}C compilation

Regarding the ^{14}C results of the calendar years of α -cellulose extracts from the native *C. odorata* growing in the equatorial Amazon, two of the eight samples were from calendar years dated to the time period before the onset of the thermonuclear bomb tests. The remaining six samples were from calendar years between 1955 and 2005. Triplicate ^{14}C results were produced from the material belonging to the calendar years of 1956, 1960, and 1969, and duplicates were produced for all others (19 radiocarbon results in total). All ^{14}C signatures of *C. odorata* tree rings matched with the dendrochronological dates, including those pertaining to the pre-bomb period (Fig. 6).

Table 2

Results of the ^{14}C analysis for reference materials after the LDEO α -cellulose extraction. The average and standard deviations (SD) of ^{14}C values are shown, followed by their respective radiocarbon ages. Number of replications and average cellulose yields, defined as mass % of the original sample after extraction, are also shown for every organic material tested (when applicable).

Ref. Material	$F^{14}\text{C}$	\pm stdev	^{14}C age ^a	\pm SD	# of rep.	% yield
Queets-A	0.0071	0.0020	40000	2300	6	0.2
AVR-07-Pal37	0.0091	0.0008	37800	740	9	2.2
FIRI-D	0.5696	0.0014	4520	20	5	25
FIRI-H	0.7560	0.0016	2240	15	7	25
FIRI-J	1.1061	0.0018	Modern	–	9	10
IAEA-C3	1.2967	0.0031	Modern	–	15	N/A

^a Radiocarbon ages labeled “Modern” are associated with samples that contain excess ^{14}C from mid-20th-century atmospheric thermonuclear weapons tests.

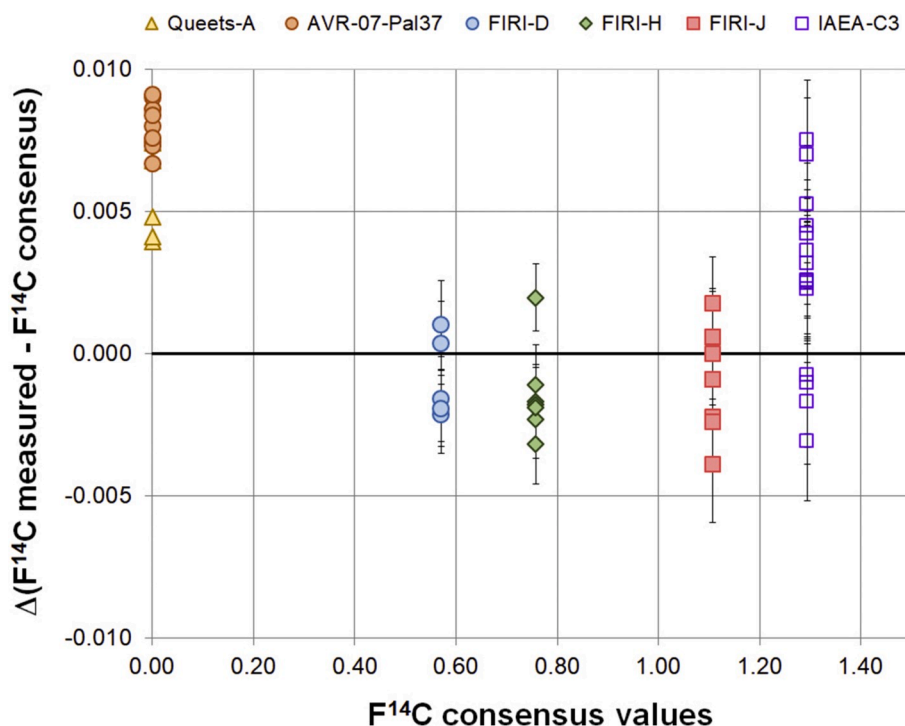


Fig. 4. Plot shows differences in individual $F^{14}\text{C}$ measurements shown in Table 2 against consensus values reported in Table 1. Replicated ^{14}C values and one-sigma uncertainty are from multiple units or subsamples of the materials extracted using the LDEO protocol. Individual $F^{14}\text{C}$ values of reference materials were fully corrected using the average values of the blanks (i.e., Queets-A and AVR-07-Pal37, as reported in Table 2), spectrometer $^{13}\text{C}/^{12}\text{C}$ data, and normalization by primary standards, as described in the text. Residual $F^{14}\text{C}$ values of blanks are positive, as they are not being corrected by their own average ^{14}C signatures. For details on the proficiency testing performed in this study, refer to Table 2.

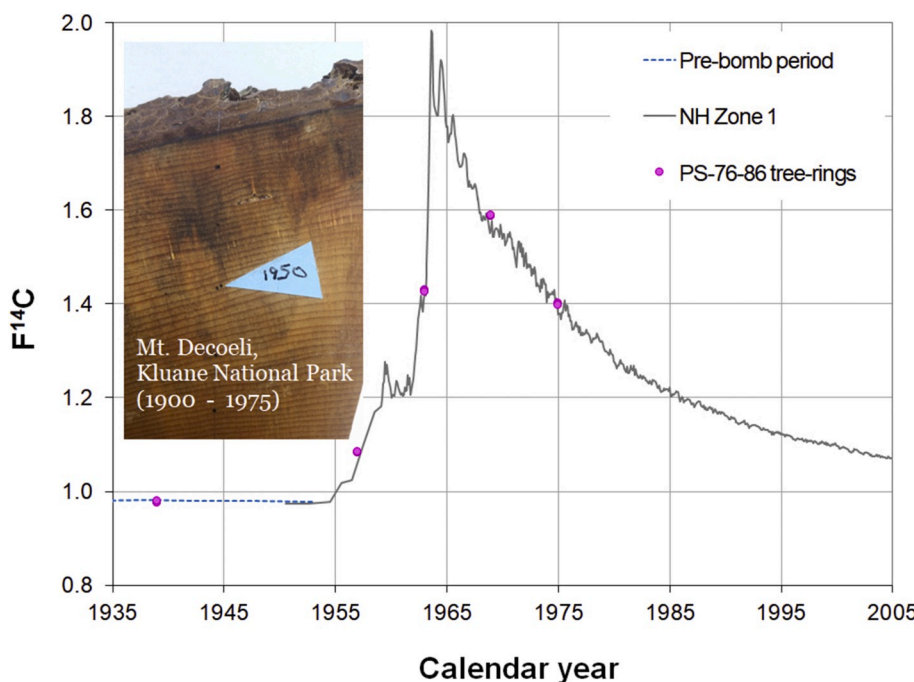


Fig. 5. Plot shows individual $F^{14}\text{C}$ values of selected annual tree ring samples (pink circles) of whole wood from a Canadian PS-76-86 wood wedge. In all cases error bars are smaller than symbols. Here, calendar dates for ^{14}C results from duplicates overlap and cannot be discriminated. Individual results are shown in Table 3. Monthly $F^{14}\text{C}$ values of atmospheric CO_2 from NH Zone 1 (1950–2005) are represented by a solid line (Hua et al., 2013). A short sequence of the pre-bomb period (dashed blue line) is also shown. No sub-annual radial growth correction was applied to the calendar years attained by a simple visual inspection of the wood wedge. An image of the PS-76-86 wood cross-section wedge is provided. (For interpretation of the references to color in this figure legend, the reader is referred to the Web version of this article.)

Because the dendrochronological techniques provide a calendar year without an associated season/month and the ^{14}C curves are built using monthly and reconstructed monthly values from tree rings (Hua et al., 2013), for direct comparisons the dendrochronological calendar dates were adjusted to the calendar's sub-annual level based on the estimated growth period shown in Fig. 2. A decimal time fraction correction of 0.4 ± 0.2 yrs was added to the dendrochronological dates, which pointed to the time of peaked tissue growth: April. Although there is still some room for a small displacement in either direction of the x-axis (Fig. 6), the assignation of the *C. odorata* dendrochronology dates by a decimal

calendar year in the middle of the growing season (optimum timing of $^{14}\text{CO}_2$ fixation through photosynthesis) places this tree-ring ^{14}C dataset perfectly in phase with the Southern Hemisphere Zone 3 (Hua et al., 2013). Regarding the NSC, again no transport of previous years' NSC in wood tissue (Cain and Suess, 1976) was observed in the ^{14}C results from the calendar years of 1940 and 1946 (Fig. 6).

To determine whether both the dendrochronological record of *C. odorata* of Paru State Forest and our techniques discussed above can be used to fine-tune future atmospheric ^{14}C compilations, we performed sensitive analysis based on the several ^{14}C replicates of tree-ring samples

Table 3

Average and standard deviations (SD) of the ^{14}C values (F^{14}C) of 5 tree rings dated to calendar years sampled from a cross-dated Canadian wood wedge.

PS-76-86 calendar years	UCIAMS#	F^{14}C	$\pm 1\sigma$	Av. F^{14}C	$\pm \text{SD}$
1939 (1)	207352	0.9750	0.0016	0.9768	0.0025
1939 (2)	207353	0.9786	0.0015		
1957 (1)	219672	1.0828	0.0018	1.0837	0.0013
1957 (2)	219673	1.0847	0.0024		
1962 (1)	219674	1.4283	0.0025	1.4271	0.0017
1962 (2)	219675	1.4259	0.0025		
1969 (1)	219676	1.5864	0.0038	1.5878	0.0019
1969 (2)	219678	1.5891	0.0029		
1975 (1)	219679	1.4016	0.0025	1.3992	0.0034
1975 (2)	219680	1.3967	0.0025		

Measurement lab code is indicated by UCIAMS#.

measured. A standard deviation was calculated using a separate pool of the *C. odorata* ^{14}C results and yielded 2.2‰, indicating that our overall procedure (from separation of tree rings to graphite target measurement) has a good to excellent reproducibility level. The precision within each year's replicates ranged from ± 0.4 to $\pm 2.3\text{‰}$ (Table 4), except for the year 1964, which showed a larger discrepancy ($\pm 4.3\text{‰}$). This discrepancy may be explained by the rapid changes in ^{14}C signatures that occurred along the months during this particular year (i.e., 1964), which can be observed in atmospheric $^{14}\text{CO}_2$ in both hemispheres: in NH (gray curve in Fig. 6) as well as in SH (blue curve in Fig. 6). Therefore, the ^{14}C signatures may differ depending largely on when the organic tissue was formed, early or late in the growing season. Since replicated samples were done by initially subsampling wood fibers into two Eppendorfs™ prior to the cellulose extraction proceedings and thus before the ultrasound homogenization proceeding (Andreu-Hayles et al., 2019), we suspect that the scattered result associated with 1964 could be the result of these two factors (i.e., large ^{14}C atmospheric variation at a sub-annual level coupled with unintended selection of sub-annual cellulose fibers).

Finally, accuracy was further evaluated by the alignment between the *C. odorata* calendar years and ^{14}C ages after calibration using the

software CALIBomb (Fig. 7). Note that the result associated with the calendar year 1999 appears to be slightly off of the 1:1 line when ^{14}C age calibration was obtained with the SH Zone 3 curve of Hua et al. (2013), but a bit better when the Minas Gerais, Brazil dataset (22°S; Santos et al., 2015) is used for the two calendar years of 1969 and 1979 (blue line in Fig. 7; data in Table 4). In the Hua et al. (2013) compilation, atmospheric ^{14}C between January 1973 and March 2011 was calculated based on extended monthly datasets from sites located at higher latitudes, such as Wellington in New Zealand (41°S; Currie et al., 2011; Brailsford and Nichol, 2012). Therefore, we suspect that the difference may be associated with variations due to latitudinal sources and sinks in land (Krakauer et al., 2006), especially from middle to lower latitudes, where crucial high-precision ^{14}C data over South America is still lacking (Santos et al., 2019). Unfortunately, the Minas Gerais dataset of Santos et al. (2015) is too short to provide further atmospheric ^{14}C variation information beyond 1998, and just two calendar years (1969 and 1979) were calibrated using this record (Table 4). Nonetheless, the correlation between ^{14}C calibrated ages and cross-dating dates are excellent on the overlapping period (Fig. 7). This straightforward visualization of the data further confirms that this Eastern Equatorial Amazon tree species forms annual rings and that the dendrochronological cross-dating techniques applied successfully provide a correct calendar year for the tree rings analyzed.

Considering the excellent agreement between the ^{14}C signatures of all tree rings analyzed and the ^{14}C curve of SH Zone 3 within uncertainties of $\pm 1\text{yr}$ (i.e., for BPD method), it can be concluded that the *C. odorata* chronology of Granato-Souza et al. (2018a) from 1786 to 2016 exhibits annual resolution as a result of a seasonal cambial dormancy of annual growth.

4. Summary and future directions

To ensure that the recently implemented LDEO α -cellulose extraction protocol (Andreu-Hayles et al., 2019) can be used for materials destined for ^{14}C analyses, an assessment through well-known and frequently used ^{14}C reference materials was performed. The ^{14}C results from a large

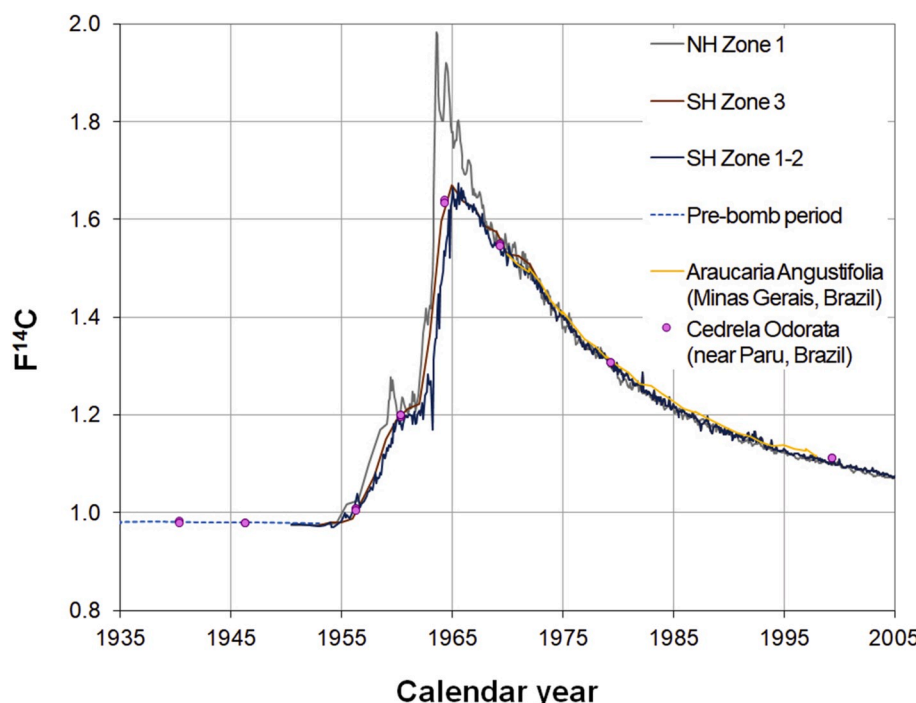


Fig. 6. F^{14}C of *C. odorata* tree-ring samples (pink circles) compared to the ^{14}C values of atmosphere in the SH Zone 3 (dark brown line, dataset from Hua et al., [2013]). The pre-bomb period (light blue dashed line) was based on datasets produced from ^{14}C values reported by McCormac et al. (1998, 2002), as well as Hogg et al. (2002) from tree rings of New Zealand and South Africa, respectively. The current atmospheric ^{14}C curves of NH Zone 1 and SH Zones 1–2 are also shown to corroborate the differences from all datasets. The Minas Gerais dataset (Santos et al., 2015), based on a single annual tree ring/ ^{14}C record from South America (yellow solid line), is also shown for reference. Here, the dendrochronological calendar ages were adjusted by $0.4 \pm 0.2\text{ yrs}$ (see text for details). All 19 F^{14}C values were plotted. Note that besides the excellent agreement with SH Zone 3, most of the F^{14}C replicate values overlapped, which can make it difficult to differentiate between individual values. Individual uncertainties are smaller than symbols. (For interpretation of the references to color in this figure legend, the reader is referred to the Web version of this article.)

Table 4

^{14}C of *C. odorata* tree-ring samples from eight specific calendar years are shown followed by averaged and standard deviations ($\pm\text{SD}$) of replicates measured. Best fit CALIBomb age range for averaged ^{14}C data based on $\pm 1\sigma$ output is also shown, using two datasets (when applicable). Pooled $\pm\text{SD}$ of 2.2‰ (details in text) was used as individual uncertainty input for each averaged ^{14}C data calibrated by the CALIBomb program. Radiocarbon record used to calibrate averaged ^{14}C data and their associated citations are provided to illustrate small differences in calibrated ^{14}C age ranges.

Dendro dates	UCIAMS#	^{14}C	Averaged ^{14}C	$\pm\text{SD}$	CALIBomb calibrated ^{14}C ages ($\pm 1\sigma$)	Dataset used
1940	215227	0.9767	0.9764	0.0006	–	N/A
	207362	0.9769				
	215228	0.9758				
1946	207363	0.9777	0.9775	0.0004	–	N/A
	207364	0.9772				
1956	207365	1.0068	1.0060	0.0020	1956.29–1956.49 cal AD	SHZ3 (Hua et al., 2013)
	207366	1.0074				
	207367	1.0037				
1960	207368	1.1945	1.1971	0.0023	1960.10–1960.52 cal AD	SHZ3 (Hua et al., 2013)
	207369	1.1985				
	207370	1.1984				
1964	207371	1.6383	1.6352	0.0043	1964.45–1964.60 cal AD	SHZ3 (Hua et al., 2013)
	207372	1.6322				
1969	207373	1.5488	1.5474	0.0021	1969.46–1969.74 cal AD	SHZ3 (Hua et al., 2013) Minas Gerais, Brazil (Santos et al., 2015)
	207374	1.5484			1968.85–1969.12 cal AD	
	207375	1.5450				
1979	207376	1.3059	1.3064	0.0007	1979.05–1979.89 cal AD	SHZ3 (Hua et al., 2013) Minas Gerais, Brazil (Santos et al., 2015)
	207377	1.3069			1979.37–1979.79 cal AD	
1999	207378	1.1100	1.1098	0.0003	1996.90–1998.70 cal AD	SHZ3 (Hua et al., 2013)
	207379	1.1096				

UCIAMS# corresponds to measurement lab code. The Minas Gerais, Brazil record found in CALIBomb runs from 1927 to 1997.

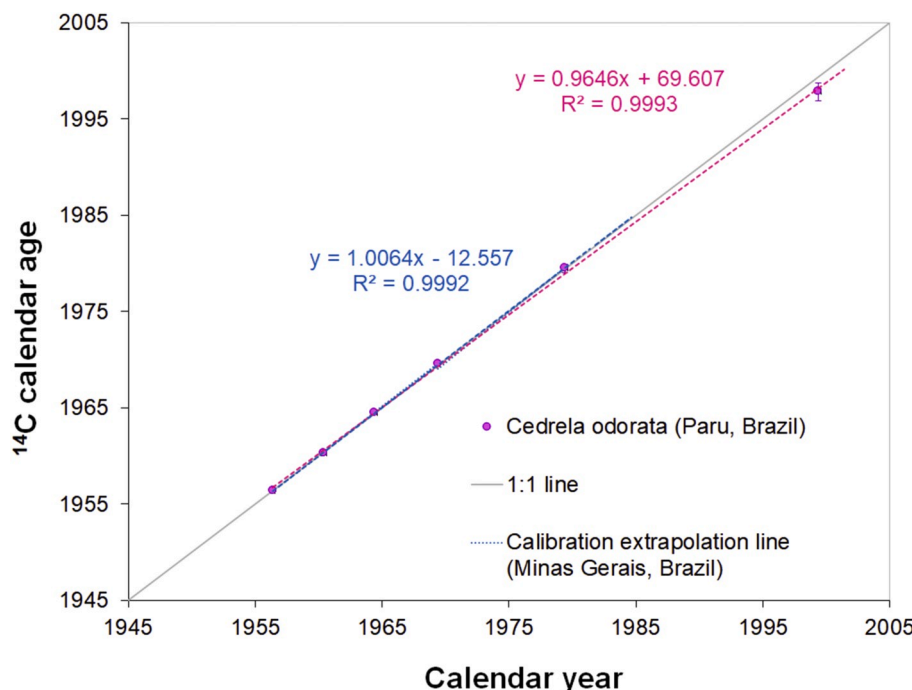


Fig. 7. Comparison of dendrochronological calendar years of *C. odorata* and calibrated ^{14}C BPD ages using the software CALIBomb (<http://intcal.qub.ac.uk/CALIBomb>) and two datasets: a) SH Zone 3 of Hua et al. (2013) for all six post-bomb calendar years (dashed pink linear regression); and b) Minas Gerais of Santos et al. (2015) for the calendar years of 1969 and 1979, followed by SH Zone 3 of Hua et al. (2013) for all others (dashed blue linear regression, which stops at 1985). For ^{14}C calendar age calibration purposes, we used the relative error determined by pooled standard deviation of replicates measured (i.e., $\pm 2.2\text{\textperthousand}$; see text for details). Except for the calendar age of 1956, averaged ^{14}C values yielded several possibilities for ^{14}C calendar years. Thus, we determined the most likely result for each ^{14}C value/calendar year pair, as calendar years were predetermined by dendrochronological techniques (Table 4). Results in very close proximity to the diagonal 1:1 line indicate that a match between calendar ages assigned by dendrochronology and ^{14}C has been found. (For interpretation of the references to color in this figure legend, the reader is referred to the Web version of this article.)

number of reference materials, covering the entire discernible ^{14}C signature range, were basically indistinguishable from consensus values within expected uncertainties, indicating that this extraction method is suitable for high-precision ^{14}C -AMS dating. Moreover, the Andreu-Hayles et al. (2019) cellulose extraction system is a step forward toward attaining α -cellulose samples destined for ^{14}C analyses with reduced preparation time. Its regular implementation can potentially expedite sample processing, and in principle reduce the expensive costs of this kind of analysis, as chemical expenditures also can be minimized.

Regarding annual periodicity of the *C. odorata* from the Paru State Forest (Granato-Souza et al., 2018a), remarkably close matches between cellulose extracts of eight dendrochronologically-dated tree rings and

their ^{14}C signatures were found by comparing these results directly to the atmospheric ^{14}C SH Zone 3 dataset (Hua et al., 2013) and the Minas Gerais, Brazil, dataset of Santos et al. (2015). Hence, by relating the ^{14}C signal measured in tree-ring tissue of a known calendar year with post-bomb- ^{14}C records, we can confirm that the tree rings in this dendrochronological record have an annual growth signal.

Through strict quality control measurements of reference materials and replication of data by the ^{14}C BPD, we showed the potential for tree-ring studies within the ITCZ band. More specifically, the rigorous assessment of the dendrochronologically-dated *C. odorata* record from the Eastern Equatorial Amazon (as illustrated here) allowed us to select this tree species to produce a lower-latitude ^{14}C record ($\sim 1^\circ\text{S}$). Yet such

a record remains all but nonexistent. Santos et al. (2019) proposed to extend the observational record by developing annually resolved atmospheric post-AD 1950 ^{14}C data using cellulose material from rigorous dendrochronologically-dated tree rings across the ITCZ band. Newly developed tree-ring ^{14}C datasets would then be modelled in order to spatially and temporally expand global atmospheric $^{14}\text{CO}_2$. Moreover, the current atmospheric ^{14}C compilation stops at about 2010 (Hua et al., 2013). While Wellington routinely updates atmospheric $^{14}\text{CO}_2$ in SH (Turnbull et al., 2017), once the *C. odorata* dendrochronology reconstruction is fully reproduced by ^{14}C dating of tree rings, recent atmospheric ^{14}C variations at very distinctive SH latitudes will be possible. Therefore, we plan to measure the *C. odorata* from the Eastern Equatorial Amazon record ring by ring, from 1940 to 2016, to generate a complete tree-ring ^{14}C dataset to be included in a future global atmospheric ^{14}C compilation.

Acknowledgements

This research was supported by the Keck Carbon Cycle Accelerator Mass Spectrometry Laboratory at UCI through GMS, and U.S. National Science Foundation (NSF) grants AGS-1703035 and AGS-1903690. We would also like to acknowledge through LAH Columbia University's Center for Climate, the U.S. National Science Foundation (NSF) grants AGS-1702789, OISE- 1743738, and PLR-1504134, and the project THEMES supported by the BNP-Paribas Foundation. We also appreciate the help of Jessie Geary for her technical assistance in sample processing at LDEO. Graphite sample preparations and analysis were performed with the help of Malissa Tayo, Shawn Pedron, and Xiaomei Xu at UCI. DG and ACCB give special thanks to Dr. David W. Stahle and the U.S. National Science Foundation grants (NSF 13-576), which allowed the collection and paid for all the logistics involved in transporting the wood cross-sections to the dendrochronology laboratory located at the Federal University of Lavras in Brazil, and for the invaluable work done at the Laboratory of Dendrochronology at the University of Arkansas. DG was funded by the Coordination for the Improvement of Higher Education Personnel (CAPES). We gratefully acknowledge the generosity of Evandro Dalmaso, the owner of CEMAL logging company, which provided logistical support and wood donations for the execution of this study. The LDEO contribution number is # 8397.

References

Adams, H.D., Zeppel, M.J., Anderegg, W.R., Hartmann, H., Landhäusser, S.M., Tissue, D.T., Huxman, T.E., Hudson, P.J., Franz, T.E., Allen, C.D., Anderegg, L.D., 2017. A multi-species synthesis of physiological mechanisms in drought-induced tree mortality. *Nat. Ecol. Evol.* 1 (9), 1285.

Anchukaitis, K.J., Evans, M.N., Lange, T., Smith, D.R., Leavitt, S.W., Schrag, D.P., 2008. Consequences of a rapid cellulose extraction technique for oxygen isotope and radiocarbon analyses. *Anal. Chem.* 80 (6), 2035–2041.

Andreu-Hayles, L., Santos, G.M., Herrera-Ramírez, D.A., Martín-Fernández, J., Ruiz-Carrascal, D., Boza-Espinoza, T.E., Fuentes, A.F., MJ, P., 2015. Matching dendrochronological dates with the Southern Hemisphere 14 C bomb curve to confirm annual tree rings in *Pseudolmedia rigida* from Bolivia. *Radiocarbon* 57 (1), 1–13. https://doi.org/10.2458/azu_rc.57.18192.

Andreu-Hayles, L., Levesque, M., Martín-Benito, D., Huang, W., Harris, R., Oelkers, R., Leland, C., Martín-Fernández, J., Anchukaitis, K.J., Helle, G., 2019. A high yield cellulose extraction system for small whole wood samples and dual measurement of carbon and oxygen stable isotopes. *Chem. Geol.* 504, 53–65. <https://doi.org/10.1016/j.chemgeo.2018.09.007>.

Baker, J.C., Santos, G.M., Brienen, R.J., 2017. Does *Cedrela* always form annual rings? Testing ring periodicity across South America using radiocarbon dating. *Trees* 31 (6), 1999–2009. <https://doi.org/10.1007/s00468-017-1604-9>.

Beramendi-Oroso, L.E., Johnson, K.R., Noronha, A.L., González-Hernández, G., Villanueva-Díaz, J., 2018. High precision radiocarbon concentrations in tree rings from Northeastern Mexico: a new record with annual resolution for dating the recent past. *Quat. Geochronol.* 48, 1–6.

Beverly, R.K., Beaumont, W., Tauz, D., Ormsby, K.M., von Reden, K.F., Santos, G.M., Southon, J.R., 2010. The Keck carbon cycle AMS laboratory, university of California, irvine: status report. *Radiocarbon* 52 (2), 301–309.

Biondi, F., Fessenden, J.E., 1999. Radiocarbon analysis of *Pinus lagunae* tree rings: implications for tropical dendrochronology. *Radiocarbon* 41 (3), 241–249.

Board, O.S., National Research Council, 2002. Chemical Reference Materials: Setting the Standards for Ocean Science. National Academies Press.

Brailsford, G., Nichol, S., 2012. NIWA Baring Head (Wellington)Δ14C Data from December 1954 to March 2011. World Data Centre for Greenhouse Gases. <ftp://ftp.niwa.co.nz/tropac/>.

Brauning, A., Volland-Voigt, F., Burchardt, I., Ganzhi, O., Nauss, T., Peters, T., 2009. Climatic control of radial growth of *Cedrela Montana* in a humid mountain rainforest in southern Ecuador. *Erdkunde* 63 (4), 337–345.

Brienen, R.J.W., Schöngart, J., Zuidema, P.A., 2016. Tree rings in the tropics: insights into the ecology and climate sensitivity of tropical trees. In: Goldstein, G., Santiago, L.S. (Eds.), *Tropical Tree Physiology. Adaptations and Responses in a Changing Environment*. Springer International Publishing, Switzerland, pp. 439–461.

Cain, W.F., Suess, H.E., 1976. Carbon 14 in tree rings. *J. Geophys. Res.* 81 (21), 3688–3694.

Currie, K.I., Brailsford, G., Nichol, S., Gomez, A., Sparks, R., Lassey, K.R., Riedel, K., 2011. Tropospheric $^{14}\text{CO}_2$ at Wellington, New Zealand: the world's longest record. *Biogeochemistry* 104 (1–3), 5–22.

de Miranda, D.L.C., Higuchi, N., Trumbore, S.E., Latorraca, J.V.F., do Carmo, J.F., Lima, A.J., 2018. Using radiocarbon-calibrated dendrochronology to improve tree-cutting cycle estimates for timber management in southern Amazon forests. *Trees* 32 (2), 587–602.

Douglass, A.E., 1941. Cross dating in dendrochronology. *J. For.* 39, 825–831.

Dünisch, O., Ribeiro Montóia, V., Bauch, J., 2003. Dendroecological investigations on *Swietenia macrophylla* King and *Cedrela odorata* L. (Meliaceae) in the central Amazon. *Trees* 17, 244–250. <https://doi.org/10.1007/s00468-002-0230-2>.

Fichtler, E., Clark, D.A., Worbes, M., 2003. Age and long-term growth of trees in an old-growth tropical rain forest, based on analyses of tree rings and ^{14}C . *Biotropica* 35 (3), 306–317.

Fritts, H.C., 2001. *Tree Rings and Climate*. Academic Press INC, London.

Furze, M.E., Huggett, B.A., Aubrecht, D.M., Stoltz, C.D., Carbone, M.S., Richardson, A.D., 2019. Whole-tree nonstructural carbohydrate storage and seasonal dynamics in five temperate species. *New Phytol.* 221 (3), 1466–1477.

Garreaud, R.D., Vuille, M., Compagnucci, R., Marengo, J., 2009. Present day South American climate. *Palaeogeogr. Palaeoclimatol. Palaeoecol.* 281, 180–195.

Geraldo Jimenez, J.A., del Valle, J.I., 2011. Estudio del crecimiento de *Priacaria copaifera* (Caesalpinaeae) mediante técnicas dendrocronológicas. *Rev. Biol. Trop.* 59 (4), 1813–1831.

Granato-Souza, D., Stahle, D.W., Barbosa, A.C., Feng, S., Torbenson, M.C., de Assis Pereira, G., Schöngart, J., Barbosa, J.P., Griffin, D., 2018a. Tree rings and rainfall in the equatorial Amazon. *Clim. Dynam.* 1–13 <https://doi.org/10.1007/s00382-018-4227-y>.

Granato-Souza, D., Pereira, G.A., Stahle, D.W., Barbosa, A.C., 2018b. NOAA/WDS Paleoclimatology - Granato-Souza - Rio Paru Site A - CESP - ITRDB BRA001, 2018-05-14. NOAA National Centers for Environmental Information.

Granato-Souza, D., Stahle, D.W., Torbenson, M.C.A., Howard, I.M., Barbosa, A.C., Feng, S., Schongart, J., 2020. Multi-decadal changes in wet season precipitation totals over the eastern Amazon. *Geophys. Res. Lett.* <https://doi.org/10.1029/2020GL087478>.

Griffin, R.D., Woodhouse, C.A., Meko, D.M., Stahle, D.W., Faulstich, H.L., Carrillo, C., Touchan, R., Castro, C.L., Leavitt, S.W., 2013. North American monsoon precipitation reconstructed from tree rings. *Geophys. Res. Lett.* <https://doi.org/10.1002/grl.50184>.

Groenendijk, P., Sass-Klaassen, U., Bongers, F., Zuidema, P.A., 2014. Potential of tree-ring analysis in a wet tropical forest: a case study on 22 commercial tree species in Central Africa. *For. Ecol. Manag.* 323, 65–78.

Hadad, M.A., Santos, G.M., Alejandro RoigJuárez, Grainger, F., CSG, 2015. Annual nature of the growth rings of *Araucaria araucana* confirmed by radiocarbon analysis. *Quat. Geochronol.* 30, 42–47. <https://doi.org/10.1016/j.quageo.2015.05.002>.

Haines, H.A., Olley, J.M., English, N.B., Hua, Q., 2018. Anomalous ring identification in two Australian subtropical Araucariaceae species permits annual ring dating and growth-climate relationship development. *Dendrochronologia* 49, 16–28.

Herrera-Ramírez, D., Andreu-Hayles, L., delValle, J.I., Santos, G.M., Gonzalez, P.L., 2017. Nonannual tree rings in a climate-sensitive *Priacaria copaifera* chronology in the Atrato River, Colombia. *Ecol. Evol.* 7 (16), 6334–6345.

Hogg, A.G., McCormac, F.G., Higham, T.F., Reimer, P.J., Baillie, M.G., Palmer, J.G., 2002. High-precision radiocarbon measurements of contemporaneous tree-ring dated wood from the British Isles and New Zealand: AD 1850e1950. *Radiocarbon* 44 (3), 633–640.

Holmes, R.L., 1983. Computer-assisted quality control in tree-ring dating and measurement. *Tree-Ring Bull.* 44, 69–78.

Hua, Q., Barbetti, M., Levchenko, V.A., D'Arrigo, R.D., Buckley, B.M., Smith, A.M., 2012. Monsoonal influence on southern hemisphere $^{14}\text{CO}_2$. *Geophys. Res. Lett.* 39 (19), L19806. <https://doi.org/10.1029/2012GL052971>.

Hua, Q., Barbetti, M., Rakowski, A., 2013. Atmospheric radiocarbon for the period 1950–2010. *Radiocarbon* 55 (4), 2059–2072.

Krakauer, N.Y., Randerson, J.T., Primeau, F.W., Gruber, N., Menemenlis, D., 2006. Carbon isotope evidence for the latitudinal distribution and wind speed dependence of the air-sea gas transfer velocity. *Tellus B: Chem. Phys. Meteorol.* 58 (5), 390–417. <https://doi.org/10.1111/j.1600-0889.2006.00223.x>.

Kutschera, W., 2018. Applications of ^{14}C , the most versatile radionuclide to explore our world. In: The Euroschool on Exotic Beams, vol. 5. Springer, Cham, pp. 1–30.

Leavitt, S.W., Bannister, B., 2009. Dendrochronology and radiocarbon dating: the laboratory of tree-ring research connection. *Radiocarbon* 51 (1), 373–384.

Leavitt, S.W., Danzer, S.R., 1993. Method for batch processing small wood samples to holocellulose for stable-carbon isotope analysis. *Anal. Chem.* 65 (1), 87–89.

Levin, I., Hesshaimer, V., 2000. Radiocarbon—A unique tracer of global carbon cycle dynamics. *Radiocarbon* 42, 69–80.

Levin, I., Hammer, S., Kromer, B., Meinhardt, F., 2008. Radiocarbon observations in atmospheric CO₂: determining fossil fuel CO₂ over Europe using Jungfraujoch observations as background. *Sci. Total Environ.* 391, 211–216.

Levin, I., Kromer, B., Hammer, S., 2013. Atmospheric D14CO₂ trend in Western European background air from 2000 to 2012. *Tellus B* 65, 20092. <https://doi.org/10.3402/tellusb.v65i0.20092>.

Lopez, L., Villalba, R., 2011. Climate influences on the radial growth of *Centrolobium microchaete*, a valuable timber species from tropical dry forests in Bolivia. *Biotropica* 43, 41–49. <https://doi.org/10.1111/j.1744-7429.2010.00653.x>.

López, L., Stahle, D., Villalba, R., Torbenson, M., Feng, S., Cook, E., 2017. Tree-ring reconstructed rainfall over the southern Amazon basin. *Geophys. Res. Lett.* 44, 7410–7418. <https://doi.org/10.1002/2017GL073363>.

Marengo, J.A., Espinoza, J.C., 2016. Extreme seasonal droughts and floods in Amazonia: causes, trends and impacts. *Int. J. Climatol.* 36, 1033–1050. <https://doi.org/10.1002/joc.4420>.

Marengo, J.A., Soares, W.R., 2004. Climatology of the low-level jet east of the andes as derived from the NCEP–NCAR reanalyses: characteristics and temporal variability. *J. Clim.* 17, 2261–2280.

McCormac, F.G., Hogg, A.G., Higham, T.F.G., Lynch-Stieglitz, J., Broecker, W.S., Baillie, M.G.L., Palmer, J., Xiong, L., Pilcher, J.R., Brown, D., Hoper, S.T., 1998. Temporal variation in the interhemispheric C-14 offset. *Geophys. Res. Lett.* 25, 1321–1324.

McCormac, F.G., Reimer, P.J., Hogg, A.G., Higham, T.F.G., Baillie, M.G.L., Palmer, J., Stuiver, M., 2002. Calibration of the radiocarbon time scale for the Southern Hemisphere: AD 1850–950. *Radiocarbon* 44, 641–651.

McNaught, A.D., Wilkinson, A., 1997. Compendium of Chemical Terminology, second ed. BlackwellScientific, Oxford.

Nobre, A.D., 2014. The Future Climate of Amazonia. Scientific Assessment Report Sponsored by CCST-INPE, INPA and ARA. São José dos Campos, Brazil, p. 42pp.

Novak, K., De Luis, M., Saz, M.A., Longares, L.A., Serrano-Notivoli, R., Ravnitos, J., Ćufar, K., Gricar, J., DiFilippo, A., Piovesan, G., Rathgeber, C.B., 2016. Missing rings in *Pinus halepensis*—the missing link to relate the tree-ring record to extreme climatic events. *Front. Plant Sci.* 7, 727.

Ohashi, S., Durgante, F.M., Kagawa, A., Kajimoto, T., Trumbore, S.E., Xu, X., Ishizuka, M., Higuchi, N., 2016. Seasonal variations in the stable oxygen isotope ratio of wood cellulose reveal annual rings of trees in a Central Amazon terra firme forest. *Oecologia* 180 (3), 685–696.

Pearson, S., Hua, Q., Allen, K., Bowman, D.M., 2011. Validating putatively cross-dated *Callitris* tree-ring chronologies using bomb-pulse radiocarbon analysis. *Aust. J. Bot.* 59 (1), 7–17.

Reimer, P.J., Brown, T.A., Reimer, R.W., 2004. Discussion: reporting and calibration of post-bomb 14C data. *Radiocarbon* 46 (3), 1299–1304.

Reyes, A.V., Froese, D.G., Jensen, B.J., 2010. Permafrost response to last interglacial warming: field evidence from non-glaciated Yukon and Alaska. *Quat. Sci. Rev.* 29 (23–24), 3256–3274.

Rozanski, K., Stichler, W., Gonfiantini, R., Scott, E.M., Beukens, R.P., Kromer, B., Van Der Plicht, J., 1992. The IAEA 14C intercomparison exercise 1990. *Radiocarbon* 34, 506–519.

Rozendaal, D.M.A., Zuidema, P.A., 2011. Dendroecology in the tropics: a review. *Trees* 25, 3–16. <https://doi.org/10.1007/s00468-010-0480-3>.

Santos, G.M., 2012. Beyond archaeology: 14C-AMS and the global carbon cycle. AIP Conference Proceedings 1423 (1), 311–318.

Santos, G.M., Ormsby, K., 2013. Behavioral variability in ABA chemical pretreatment close to the 14C age limit. *Radiocarbon* 55 (2–3), 534–544.

Santos, G.M., Xu, X., 2017. Bag of tricks: a set of techniques and other resources to help 14C laboratory setup, sample processing, and beyond. *Radiocarbon* 59 (3), 785–801.

Santos, G.M., Moore, R., Southon, J., Griffin, S., Hinger, E., Zhang, D., 2007. AMS 14C preparation at the KCCAMS/UCI Facility: status report and performance of small samples. *Radiocarbon* 49 (2), 255–269.

Santos, G.M., Southon, J.R., Drenzek, N.J., Ziolkowski, L.A., Druffel, E., Xu, X., Zhang, D., Trumbore, S., Eglinton, T.I., Hughen, K.A., 2010. Blank assessment for ultra-small radiocarbon samples: chemical extraction and separation versus AMS. *Radiocarbon* 52 (3), 1322–1335.

Santos, G.M., Linares, R., Lisi, C.S., Tomazello Filho, M., 2015. Annual growth rings in a sample of Paraná pine (*Araucaria angustifolia*): toward improving the 14C calibration curve for the Southern Hemisphere. *Quat. Geochronol.* 25, 96–103.

Santos, G.M., Andreu-Hayles, L., Oelkers, R., De Pol-Holz, R., Hua, Q., Ferrero, M.E., Requena-Rojas, E.J., n Pucha-Cofrep, D., Patiño-Rosario, S., Brandes, A.F.N., Groenendijk, P., Barbosa, A.C.C., Granato-Souza, D., 2019. Tree-ring 14C data across the ITCZ over South America and Central Africa: filling the gaps in atmospheric post-AD1950 14C curves. Abstract presented at “Role of the IntCal radiocarbon calibration curves in Quaternary science” session. In: 20th INQUA Congress, Dublin, Ireland, July 25–31, 2019 (O-3195; ORAL).

Schöngart, J., 2008. Growth-Oriented Logging (GOL): a new concept towards sustainable forest management in Central Amazonian várzea flood plains. *Ecol. Manag.* 256, 46–58. <https://doi.org/10.1016/j.foreco.2008.03.037>.

Schöngart, J., Junk, W.J., Piedade, M.T.F., Ayres, J.M., Hüttermann, A., Worbes, M., 2004. Teleconnection between tree growth in the amazonian floodplains and the El niño–southern oscillation effect. *Global Change Biol.* 10 (5), 683–692.

Schöngart, J., Bräuning, A., Barbosa, A.C.M.C., Lisi, C.S., de Oliveira, J.M., 2017. Dendroecological studies in the neotropics: history, Status and future challenges. In: Amoroso, M., Daniels, L., Baker, P., Camarero, J. (Eds.), *Dendroecology: Ecological Studies (Analysis and Synthesis)*. Springer, pp. 35–73.

Scott, E.M., 2003. The fourth international radiocarbon intercomparison (FIRI). *Radiocarbon* 45, 135–291.

Soliz-Gamboa, C.C., Rozendaal, D., Ceccantini, G., Anygalossy, V., van der Borg, K., Zuidema, P.A., 2011. Evaluating the annual nature of juvenile rings in Bolivian tropical rainforest trees. *Trees Struct. Funct.* 25, 17–27.

Southon, J.R., Magana, A.L., 2010. A comparison of cellulose extraction and ABA pretreatment methods for AMS 14C dating of ancient wood. *Radiocarbon* 52 (3), 1371–1379.

Stahle, D.W., Burnette, D.J., Villanueva Diaz, J., Heim, R.R., Fye, F.K., Paredes, J.C., Soto, R.A., Cleaveland, M.K., 2011. Pacific and Atlantic influences on Mesoamerican climate over the past millennium. *Clim. Dynam.* 39 (6), 1431–1446.

Stahle, D.W., Cook, E.R., Burnette, D.J., Villanueva, J., Cerano, J., Burns, J.N., Griffin, D., Cook, B.I., Acuña, R., Torbenson, M.C.A., Szejner, P., Howard, I.M., 2016. The Mexican Drought Atlas: tree-ring reconstructions of the soil moisture balance during the late pre-Hispanic, colonial, and modern eras. *Quat. Sci. Rev.* 149, 34–60.

Stokes, M.A., Smiley, T.L., 1996. *An Introduction to Tree-Ring Dating*. University of Arizona Press, Tucson.

Turnbull, J.C., Mikaloff Fletcher, S.E., Brailsford, G.W., Moss, R.C., Norris, M.W., Steinkamp, K., 2017. Sixty years of radiocarbon dioxide measurements at Wellington, New Zealand: 1954–2014. *Atmos. Chem. Phys.* 17 (23), 14771–14784.

Vera, C., Higgins, W., Amador, J., Ambrizzi, T., Garreaud, R., Gochis, D., Gutzler, D., Lettenmaier, D., Marengo, J., Mechoso, C.R., Nogues-Paegle, J., Silva Dias, P.L., Zhang, C., 2006. Toward a unified view of the American monsoon systems. *J. Clim.* 19, 4977–5000.

Villalba, R., Boninsegna, J.A., Holmes, R.L., 1985. *Cedrela angustifolia* and *Juglans australis*: two new tropical species useful in dendrochronology. *Tree-Ring Bull.* 45, 25–35.

Villalba, R., Cook, E.R., Jacoby, G.C., D'Arrigo, R.D., Veblen, T.T., Jones, P.D., 1998. Tree-ring based reconstructions of northern Patagonia precipitation since AD 1600. *Holocene* 8, 659–674.

Villanueva-Diaz, J., Stahle, D.W., Luckman, B.H., Cerano-Paredes, J., Therrell, M.D., Cleaveland, M.K., Cornejo-Oviedo, E., 2007. Winter-spring precipitation reconstructions from tree rings for northeast Mexico. *Climatic Change* 83 (1–2), 117–131.

Wacker, L., Bonani, G., Friedrich, M., Hajdas, I., Kromer, B., Němec, M., Ruff, M., Suter, M., Synal, H.A., Vockenhuber, C., 2010. MICADAS: routine and high-precision radiocarbon dating. *Radiocarbon* 52 (2), 252–262.

Westbrook, J.A., Guilderson, T.P., Colinvaux, P.A., 2006. Annual growth rings in a sample of *Hymenaea courbaril*. *IAWA J.* 27 (2), 193–197.

Wils, T.H., Robertson, I., Eshetu, Z., Sassi-Klaassen, U.G., Koprowski, M., 2009. Periodicity of growth rings in *Juniperus procera* from Ethiopia inferred from crossdating and radiocarbon dating. *Dendrochronologia* 27 (1), 45–58.

Worbes, M., 1984. Periodische zuwachszonen an Bäumen zentralamazonischer überschwemmungswälder. *Naturwissenschaften* 71, 157–158.

Worbes, M., 1985. Structural and other adaptations to longterm flooding by trees in Central Amazonia. *Amazoniana* 9, 459–484.

Worbes, M., 2002. One hundred years of tree-ring research in the tropics—a brief history and an outlook to future challenges. *Dendrochronologia* 20 (1–2), 217–231.

Worbes, M., Junk, W.J., 1989. Dating tropical trees by means of 14C from bomb tests. *Ecology* 70 (2), 503–507.

Worbes, M., Staschel, R., Roloff, A., Junk, W.J., 2003. Tree ring analysis reveals age structure, dynamics and wood production of a natural forest stand in Cameroon. *For. Ecol. Manag.* 173 (1–3), 105–123.

Yoon, J.H., Zeng, N., 2010. An Atlantic influence on Amazon rainfall. *Clim. Dynam.* 34, 249–264.